Eur. Phys. J. E **6**, 91–98 (2001)

THE EUROPEAN PHYSICAL JOURNAL E

EDP Sciences

Shapes of nearly cylindrical, axisymmetric bilayer membranes

B. Božič[1,a], V. Heinrich[1,b], S. Svetina[1,2], and B. Žekš[1,2]

[1] Institute of Biophysics, Faculty of Medicine, University of Ljubljana, Lipičeva 2, SI-1000 Ljubljana, Slovenia
[2] J. Stefan Institute, Jamova 39, SI-1000 Ljubljana, Slovenia

Received 27 September 2000 and Received in final form 26 March 2001

Abstract. Shapes of nearly cylindrical sections of axisymmetric phospholipid membranes are studied theoretically. Describing the shape of such sections by their deviation from a reference cylinder, the well-established shape equation for axisymmetric bilayer membranes is expanded in terms of this deviation, and it is then solved analytically. The phase diagram shows the resulting stationary shapes as functions of system parameters and external conditions, *i.e.*, the pressure difference across the membrane, the membrane tension, the difference between the tensions of the two monolayers, and the axial force acting on the vesicle. The accuracy of the approximate analytical solution is demonstrated by comparison with numerical results. The obtained analytical solution allows to extend the analysis to include shapes where numerical methods have failed.

PACS. 87.16.-b Subcellular structure and processes – 87.16.Dg Membranes, bilayers, and vesicles – 82.70.-y Disperse systems; complex fluids

1 Introduction

A phospholipid vesicle in an aqueous medium represents the simplest system for studying the basic physical properties of membranous systems with closed surfaces. A significant such property is the equilibrium shape of a flaccid vesicle. Such shapes depend on vesicle volume, on membrane characteristics and on forces exerted on the membrane [1,2]. The equilibrium shape of an unsupported phospholipid vesicle can be predicted by the minimization [3–6] of the local and nonlocal bending contributions [7,8] to the membrane elastic energy, and of a strained vesicle by the minimization of the sum of these energies and the potential energies of the applied forces [9,10].

In many instances vesicles involve tubelike sections. Such sections represent the middle part of some vesicles with small volumes with regard to the membrane area [11]. Long tubular vesicle sections are also formed when vesicles are strained by a point force as, for instance, in tether pulling experiments [12,13]. The cylindrical membrane formations frequently occur in cells, *e.g.* as cell organelles or their interconnections [14,15]. Thus, a particular theoretical analysis of the shape behavior of tubular phospholipid vesicle sections seems to be justified.

Hitherto the occurrence of tubelike sections has been studied theoretically mostly by investigating the stability of a long cylindrically shaped membrane with respect to the deformational modes. In these studies the deformational modes are small sinusoidal deformations, along the tube and in the orthogonal direction. Ou-Yang and Helfrich analyzed [16] the stability of cylinders by considering the local bending energy with included spontaneous membrane curvature. They indicated that sufficiently negative spontaneous curvature may transform a cylinder into a tapelike form, whereas sufficiently positive spontaneous curvature may transform it into a string of beads. Bukman *et al.* [17] extended these studies by adding into the energy functional of the system the nonlocal bending term and a term representing the axial force pulling on the vesicle. They presented the phase diagram showing the domain within which a cylinder is stable, and identified the most unstable deformational modes in the domains where the cylinder is not stable.

The above stability analyses predict the shapes within the noncylindrical domains of the phase diagram only partially because the most unstable deformational modes give some indications of tubular shapes only nearby the boundaries of the cylindrical domain. However, it is of interest to reveal vesicle shape behavior within the whole range of the system's parameters. The vesicle shapes can be obtained by solving the shape equation that is the result of minimizing the corresponding energy functionals. Here, the shapes will be obtained by solving the shape equation that is based on the minimization of the membrane local and nonlocal bending energies. In particular, an analytical solution will be provided for shapes of nearly cylindrical

[a] e-mail: bojan.bozic@biofiz.mf.uni-lj.si
[b] *Present address:* Department of Biomedical Engineering, Boston University, 44 Cummington St, Boston, MA 02215, USA.

vesicle sections by taking into consideration the finite lengths of these sections. We limit ourselves to the axisymmetric shapes of tubular vesicle sections. In a complementary work, Zhang [18] recently obtained a set of nonaxisymmetric solutions of the general membrane shape equation [19] for a long tubular vesicle section where the cross-section of the obtained shapes does not vary along the section.

2 Differential equation for nearly cylindrical, axisymmetric section

The shape equation for the phospholipid vesicle is obtained by varying the sum of the local and nonlocal bending energy at given vesicle volume (V) and membrane area (A) [1,2]. The extrema of the elastic energy at given conditions correspond to the stationary shapes of the vesicle. The local bending energy (W_b) is expressed by $\frac{1}{2}k_\mathrm{c}\int(C_1+C_2-C_0)^2\mathrm{d}A$, where k_c is the bending modulus, C_1 and C_2 are the principal curvatures, and C_0 is the spontaneous membrane curvature, whereas the nonlocal bending energy (relative stretching energy, W_RE) is expressed by $\frac{k_\mathrm{r}}{2Ah^2}(\Delta A-\Delta A_0)^2$, where k_r is the nonlocal bending modulus, h is the distance between the neutral surfaces of the outer and the inner monolayer, ΔA is the difference between the areas of the outer and the inner monolayers that is equal to $h\int(C_1+C_2)\mathrm{d}A$, and ΔA_0 is the corresponding equilibrium area difference [20–22]. For a fixed distance between the poles of an axisymmetric vesicle ($\bar{Z}$) the corresponding functional is written in the form

$$\mathcal{G}=W_\mathrm{b}+W_\mathrm{RE}-\mu(V-V_0)+\lambda(A-A_0)-f(\bar{Z}-\bar{Z}_0)\,, \quad (1)$$

where μ, λ and f are the Lagrange multipliers that guarantee fixed vesicle volume, membrane area and distance between the vesicle poles ($V=V_0$, $A=A_0$ and $\bar{Z}=\bar{Z}_0$).

The variational procedure of the functional can be first performed at given ΔA, and the stationary $\mathcal{G}(\Delta A)$ dependence can be obtained. The variation of $\mathcal{G}$ with respect to ΔA gives at equilibrium ($\partial\mathcal{G}/\partial\Delta A=0$), $\partial W_\mathrm{b}/\partial\Delta A=-\mathrm{d}W_\mathrm{RE}/\mathrm{d}\Delta A$. For analysing the shape behavior of the cylindrical vesicle section, it is convenient to define the difference between the lateral tensions of the membrane monolayers ($\nu=\mathrm{d}W_\mathrm{RE}/\mathrm{d}\Delta A$), which is equal to [10]

$$\nu=\frac{k_\mathrm{r}}{Ah^2}(\Delta A-\Delta A_0)\,. \quad (2)$$

The difference between the lateral tensions is positive when the outer monolayer is more stretched than the inner one. Accordingly, the variations of $\mathcal{G}$ with respect to V, A and $\bar{Z}$, respectively, show that the pressure difference ($\mu=\partial W_\mathrm{b}/\partial V$) is defined as positive when the pressure in the vesicle is larger than in the surroundings, that the lateral tension ($\lambda=-\partial W_\mathrm{b}/\partial A$) is positive when the membrane is stretched, and that the axial force ($f=\partial W_\mathrm{b}/\partial\bar{Z}$) is positive when it stretches the vesicle along the axis.

The variation of the functional $\mathcal{G}$ with respect to the membrane shape [6,10] leads to the axisymmetric version [23] of the general membrane shape equation [19] and to the boundary condition at vesicle poles. The corresponding shape equation was presented previously (Eq. (17) of Ref. [24]) for zero spontaneous curvature. By considering also the spontaneous curvature of the bilayer (C_0), the shape equation reads

$$\begin{aligned}
&2R\sin^3\psi\,\psi'''+8R\sin^2\psi\cos\psi\,\psi''\psi'-4\sin^2\psi\cos\psi\,\psi''\\
&-R\sin\psi(\sin^2\psi-2\cos^2\psi)\psi'^3-\sin\psi(4-7\sin^2\psi)\psi'^2\\
&+\left(4C_0\sin\psi-RC_0^2+\frac{\sin^2\psi-2\cos^2\psi}{R}\right)\sin\psi\,\psi'\\
&-\left(\frac{2\lambda R}{k_\mathrm{c}}+\frac{4\nu h}{k_\mathrm{c}}\sin\psi\right)\sin\psi\,\psi'+C_0^2\sin\psi\\
&-\frac{\sin\psi(1+\cos^2\psi)}{R^2}-\frac{2\mu R}{k_\mathrm{c}}+\frac{2\lambda\sin\psi}{k_\mathrm{c}}=0\,, \quad (3)
\end{aligned}$$

where R is the distance between the symmetry axis and a point on the contour of the membrane, and ψ is the angle made by the surface normal and the symmetry axis and is defined through the relation

$$\cot\psi=-R'\,. \quad (4)$$

The prime in equations (3) and (4) denotes differentiation with respect to the position along the symmetry axis (Z). The axial force (f) appears only in the boundary condition at the two poles. In the case of the pulling force at the vesicle poles the boundary condition [24] (in the limit $R\to 0$) reads

$$\psi=-\frac{fR}{4\pi k_\mathrm{c}}\ln R\,. \quad (5)$$

Because we are looking for the shape of a nearly cylindrical axisymmetric section of the membrane, we can expand the shape equation in small deviations from the cylinder. The contour of an almost cylindrical section of the axisymmetric membrane can be expressed as

$$R(Z)=R_0+U(Z)\,, \quad (6)$$

where R_0 is the reference radius and U describes the deviation. For almost cylindrical sections ψ is approximately $\pi/2$, and thus we can, by using equations (4) and (6), expand $\sin\psi$, $\cos\psi$, ψ', ψ'' and ψ''' as a function of U. By neglecting the nonlinear terms in U, we have

$$\begin{aligned}
&\sin\psi=1\,, \qquad \cos\psi=-U'\,, \qquad \psi'=U''\,,\\
&\psi''=U'''\,, \qquad \psi'''=U^{(\mathrm{IV})}\,. \quad (7)
\end{aligned}$$

Substituting equations (6) and (7) into equation (3) and neglecting nonlinear terms, we obtain the fourth-order differential equation

$$\begin{aligned}
&R_0^4U^{(\mathrm{IV})}+\left(\frac{1}{2}-\frac{\lambda R_0^2}{k_\mathrm{c}}-\frac{2\nu hR_0}{k_\mathrm{c}}-\frac{C_0^2R_0^2}{2}+2C_0R_0\right)R_0^2U''\\
&+\left(1-\frac{\mu R_0^3}{k_\mathrm{c}}\right)U-\frac{\mu R_0^4}{k_\mathrm{c}}+\frac{\lambda R_0^3}{k_\mathrm{c}}-\frac{R_0}{2}+\frac{C_0^2R_0^3}{2}=0\,. \quad (8)
\end{aligned}$$

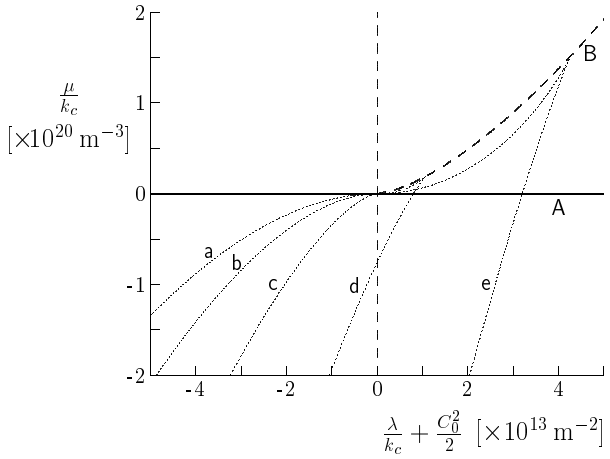

Fig. 1. The diagram shows the values of the pressure difference across the membrane (μ/k_c) and the lateral tension in the membrane ($\lambda/k_\mathrm{c}+C_0^2/2$) at which tubular sections are possible. There is one solution for the radius of the reference cylinder below curve A and there are two solutions between curves B and A. Tubular sections cannot exist for the values of the parameters out of these two regions. Curve B is obtained by setting expression (11) to zero. The dotted lines correspond to the values of the expression $\nu h/k_\mathrm{c}-C_0-f/(2\pi k_\mathrm{c}) = -8\times10^6\ \mathrm{m}^{-1}$ (a), $-4\times10^6\ \mathrm{m}^{-1}$ (b), 0 (c), $4\times10^6\ \mathrm{m}^{-1}$ (d), and $8\times10^6\ \mathrm{m}^{-1}$ (e).

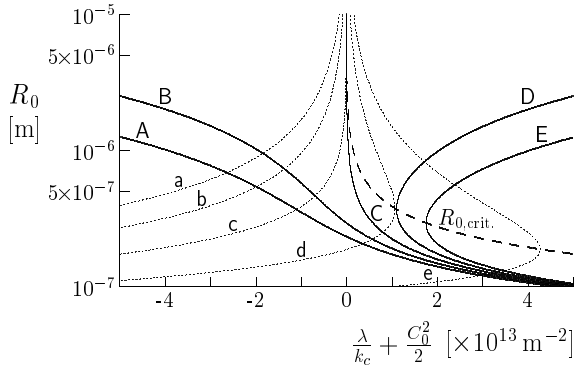

Fig. 2. The dependence of the radius of the reference cylinder (R_0) on the parameter $\lambda/k_\mathrm{c}+C_0^2/2$. The full lines represent these dependences for $\mu/k_\mathrm{c} = -4\times10^{19}\ \mathrm{m}^{-3}$ (A), $-2\times10^{19}\ \mathrm{m}^{-3}$ (B), 0 (C), $2\times10^{19}\ \mathrm{m}^{-3}$ (D), and $4\times10^{19}\ \mathrm{m}^{-3}$ (E), whereas the dotted lines represent these dependences for the expression $\nu h/k_\mathrm{c}-C_0-f/(2\pi k_\mathrm{c}) = -8\times10^6\ \mathrm{m}^{-1}$ (a), $-4\times10^6\ \mathrm{m}^{-1}$ (b), 0 (c), $4\times10^6\ \mathrm{m}^{-1}$ (d), and $8\times10^6\ \mathrm{m}^{-1}$ (e). The dashed curve shows the dependence of the critical cylinder radius on the lateral tension.

This equation shows that an ideal cylinder ($U=\mathrm{const}=0$) is a solution povided that

$$2\mu R_0^3 - 2\lambda R_0^2 + k_\mathrm{c} - k_\mathrm{c} C_0^2 R_0^2 = 0 \qquad (9)$$

is fulfilled. It is to be noted that equation (9) is equivalent to the radial equilibrium condition for the cylinder [16, 17]. Equation (9) also represents the equation to fix the reference radius R_0 in such a way that U will be small for nonideal but nearly cylindrical solutions. Once equation (9) is satisfied by our choice of R_0, we are left with a homogeneous linear differential equation for the deviation U of the shape from the reference cylinder.

Because the nearly cylindrical membrane shapes often occur in axially strained vesicles [10,25], it is appropriate to complement the present analysis by determining the interrelation between the pulling axial force and the radius of the reference cylinder. In order to obtain this interrelation we require that the correspondingly expanded third-order differential equation for the membrane shape, which is obtained by integrating equation (3) [26] and taking into account the boundary condition (Eq. (5)), is satisfied along the nearly cylindrical section up to the first order. This requirement gives the relationship between μ, λ, ν, f and the reference radius R_0 in the form

$$fR_0 + \pi\mu R_0^3 - 2\pi\lambda R_0^2 - 2\pi\nu h R_0 - \pi k_\mathrm{c}(1-C_0R_0)^2 = 0\,. \qquad (10)$$

Equation (10) can also be identified as the longitudinal equilibrium condition for the cylinder because the same equation is obtained by the variation of the corresponding thermodynamic potential for the cylinder with respect to its length [17].

3 Analytical solutions for nearly cylindrical, axisymmetric section

3.1 The reference radius of the cylindrical section

The cubic equation such as equation (9) for R_0 cannot have real and positive roots for arbitrary values of its coefficients. Therefore, it is of interest to determine at what values of the parameters a nearly cylindrical section can exist, *i.e.*, at what values of the pressure difference (μ) and lateral tension (λ) equation (9) has real, positive roots for the radius of the reference cylinder (R_0). The results of the root analysis are shown in Figures 1 and 2. Figure 1 shows that for $\mu < 0$ a single solution (*i.e.* a single real, positive root) for the reference radius exists at any λ. For $\mu > 0$, there are two solutions for the reference radius when

$$27k_\mathrm{c}\mu^2 - (2\lambda + k_\mathrm{c}C_0^2)^3 < 0\,, \qquad (11)$$

and there are no solutions for the reference radius when this condition is not fulfilled. By setting expression (11) to zero, we obtain a boundary line of the region of solutions of equation (9) (the dashed line B in Fig. 1). The two solutions for the reference radius merge at this boundary line into a single one (critical radius $R_{0,\mathrm{crit.}}$).

It is instructive to determine also the interdependence between the system parameters (μ, λ and ν) and the axial force (f) for cylinders. By eliminating R_0 from equations (9) and (10), we obtain the relationship between the pressure difference (μ), the lateral tension (λ) and the expression $\nu h/k_\mathrm{c}-C_0-f/(2\pi k_\mathrm{c})$. The values of the pressure difference and the lateral tension for some constant values of the latter expression are presented in Figure 1. At positive values of μ there are two values for the expression $\nu h/k_\mathrm{c} - C_0 - f/(2\pi k_\mathrm{c})$. That is reflected in Figure 1 by the two branches of the dotted curves d and e, of which one corresponds to the larger radius of the cylinder whereas the other to the smaller radius.

The dependence of the radius of the reference cylinder on the lateral tension is obtained by solving equation (9) for given values of μ (full lines in Fig. 2). These dependences show that the same radius can be realized at different values of the parameters. The smaller radius of the cylinder increases while the larger one decreases by decreasing λ or by increasing μ. The insertion of the obtained interdependence between μ and λ for the boundary line (expression (11) equal to zero) into equation (9) yields the dependence of the critical cylinder radius on μ or on λ, $R_{0,\mathrm{crit.}} = \sqrt[3]{k_\mathrm{c}/\mu} = \sqrt{3k_\mathrm{c}/(2\lambda + k_\mathrm{c}C_0^2)}$ (dashed line in Fig. 2). To find out the corresponding value of the expression $\nu h/k_\mathrm{c} - C_0 - f/(2\pi k_\mathrm{c})$ for a given radius of the reference cylinder and the lateral tension, we eliminate μ from equations (9) and (10) and obtain

$$\left(\frac{\lambda}{k_\mathrm{c}} + \frac{C_0^2}{2}\right) R_0^2 + 2\left(\frac{\nu h}{k_\mathrm{c}} - C_0 - \frac{f}{2\pi k_\mathrm{c}}\right) R_0 + \frac{3}{2} = 0\,. \quad (12)$$

The dependence of R_0 on the parameter $\lambda/k_\mathrm{c} + C_0^2/2$ for some values of the expression $\nu h/k_\mathrm{c} - C_0 - f/(2\pi k_\mathrm{c})$ is also shown in Figure 2 (dotted lines).

The dependence of R_0 on the parameters μ and λ for some limiting cases is instructive. For large R_0 and $\lambda \gg k_\mathrm{c}C_0^2$ the bending energy is negligible and the radius of the reference cylinder can be expressed by the law of Laplace ($R_0 = \lambda/\mu$). For small μ the radius of the reference cylinder is expressed by $R_0 = \sqrt{k_\mathrm{c}/(2\lambda + k_\mathrm{c}C_0^2)}$ where $2\lambda + k_\mathrm{c}C_0^2$ must be positive. The larger radius for the small, positive pressure difference is expressed by $R_0 = (\lambda + k_\mathrm{c}C_0^2/2)/\mu$. For small $\lambda + k_\mathrm{c}C_0^2/2$ the radius of the reference cylinder is expressed by $R_0 = \sqrt[3]{-k_\mathrm{c}/(2\mu)}$ (μ must be negative).

3.2 Types of deviations from the reference cylinder

We obtain different types of deviations from the reference cylinder by solving equation (8) that becomes, by taking into consideraton equation (9), the homogeneous linear differential equation for U. The solutions of the homogeneous differential equation for U have the form $U = Be^{ikZ}$, where the amplitude B and the wave number k are in general complex quantities. By inserting this solution into the differential equation for U, the fourth-order equation for the dimensionless product of the wave number and the reference radius (kR_0) is obtained:

$$(kR_0)^4 + \left(\frac{1}{2} - \frac{\lambda R_0^2}{k_\mathrm{c}} - \frac{2\nu h R_0}{k_\mathrm{c}} - \frac{C_0^2 R_0^2}{2} + 2C_0 R_0\right)(kR_0)^2 + \left(1 - \frac{\mu R_0^3}{k_\mathrm{c}}\right) = 0\,. \quad (13)$$

In order to express the solutions for the product kR_0 more transparently, we introduce the dimensionless lateral tension ($\bar{\lambda}$) as $(\lambda/k_\mathrm{c} + C_0^2/2)R_0^2$ and the dimensionless difference between the lateral tensions ($\bar{\nu}$) as $(\nu h/k_\mathrm{c} - C_0)R_0$. By using equation (9) and the definition for the dimensionless lateral tension, the pressure difference is a simple function of $\bar{\lambda}$ ($\mu = k_\mathrm{c}(\bar{\lambda} - 0.5)/R_0^3$). Thus, the single solution for the radius of the reference cylinder that corresponds to negative pressure differences is realized at $\bar{\lambda} < 0.5$. In the case of positive pressure differences, for the smaller radius of the cylinder the value of $\bar{\lambda}$ lies in the range between 0.5 and 1.5, while for the larger radius the value of $\bar{\lambda}$ is larger than 1.5. Namely, by rewriting equation (9) as $\lambda = \lambda(\mu, R_0)$ and differentiating this expression with respect to R_0, we obtain that for $\bar{\lambda} < 1.5$ the derivative $\mathrm{d}\lambda/\mathrm{d}R_0$ is negative, which is characteristic for the smaller radius of the cylinder (cf. Fig. 2), and for $\bar{\lambda} > 1.5$ this derivative is positive, which is characteristic for the larger radius of the cylinder. The value of $\bar{\lambda}$ for cylinders of the critical radius ($R_{0,\mathrm{crit.}}$) is 1.5.

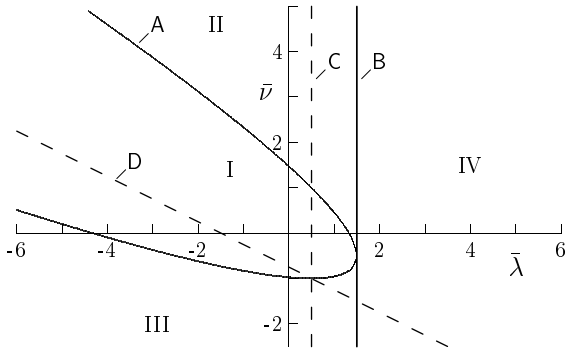

Fig. 3. The phase diagram for the shape behavior of an axisymmetric tubular membrane as a function of the dimensionless lateral tension and dimensionless difference between the lateral tensions ($\bar{\lambda}$-$\bar{\nu}$ phase diagram). The Roman numbers (from I to IV) indicate domains for which the basic functions are the ones given in the corresponding columns in Table 1. These domains are separated by curves A and B. Curve A is obtained by setting to zero the inner root of equation (14), and curve B is obtained by setting to zero equation (14) for the negative sign in front of the inner root. The pressure difference between the inner and the outer medium is positive for cylindrical sections that lie to the right of the dashed line C ($\mu = 0$ curve) and the axial force is positive for nearly cylindrical sections that lie above the dashed line D ($f = 0$ curve).

The four roots of equation (13) expressed by the dimensionless parameters are

$$kR_0 = \pm\frac{1}{2}\sqrt{1 - 2\bar{\lambda} - 4\bar{\nu} \pm \sqrt{4(\bar{\lambda} + 2\bar{\nu})^2 + 12\bar{\lambda} - 8\bar{\nu} - 23}}\,. \quad (14)$$

The obtained dependence of the wave number k on $\bar{\lambda}$, $\bar{\nu}$ and R_0 completely describes the parameter dependence of the different types of the membrane shape deviations. Namely, by the use of equation (9) we could eliminate either $\bar{\lambda}$ or R_0 from equation (14) and express the wave number k alternatively either in terms of μ, $\bar{\nu}$ and R_0 or in terms of μ, λ and ν, respectively.

The inspection of equation (14) shows that at different values of the parameters $\bar{\lambda}$ and $\bar{\nu}$ the wave numbers corresponding to the four solutions may have completely different values and character. We can identify four domains of different types of membrane shape deviations, which can be conveniently presented in a form of the phase diagram (Fig. 3). The shape of the tubular section can be

Table 1. Even (E) and odd (O) basic functions for four different types of the shape behavior of axisymmetric tubular membranes. The components of the wave numbers (α and β) and the wave numbers ($k_{\mathrm{II},1}$, $k_{\mathrm{II},2}$, $k_{\mathrm{III},1}$, $k_{\mathrm{III},2}$, $k_{\mathrm{IV},1}$ and $k_{\mathrm{IV},2}$) that appear in the basic functions are given in the legend.

domains		I	II	III	IV
basic functions	E	$\sinh\beta Z \sin\alpha Z$ $\cosh\beta Z \cos\alpha Z$	$\cosh k_{\mathrm{II},1} Z$ $\cosh k_{\mathrm{II},2} Z$	$\cos k_{\mathrm{III},1} Z$ $\cos k_{\mathrm{III},2} Z$	$\cosh k_{\mathrm{IV},2} Z$ $\cos k_{\mathrm{IV},1} Z$
	O	$\cosh\beta Z \sin\alpha Z$ $\sinh\beta Z \cos\alpha Z$	$\sinh k_{\mathrm{II},1} Z$ $\sinh k_{\mathrm{II},2} Z$	$\sin k_{\mathrm{III},1} Z$ $\sin k_{\mathrm{III},2} Z$	$\sinh k_{\mathrm{IV},2} Z$ $\sin k_{\mathrm{IV},1} Z$

$$\alpha = \frac{\sqrt{1-2\bar{\lambda}-4\bar{\nu}+\sqrt{24-16\bar{\lambda}}}}{\sqrt{8}R_0},\ \beta = \frac{\sqrt{2\bar{\lambda}+4\bar{\nu}-1+\sqrt{24-16\bar{\lambda}}}}{\sqrt{8}R_0}$$

$$k_{\mathrm{II},1} = k_{\mathrm{IV},2} = \frac{\sqrt{2\bar{\lambda}+4\bar{\nu}-1+\sqrt{4(\bar{\lambda}^2+4\bar{\nu}^2)+16\bar{\lambda}\bar{\nu}+12\bar{\lambda}-8\bar{\nu}-23}}}{2R_0}$$

$$k_{\mathrm{II},2} = \frac{\sqrt{2\bar{\lambda}+4\bar{\nu}-1-\sqrt{4(\bar{\lambda}^2+4\bar{\nu}^2)+16\bar{\lambda}\bar{\nu}+12\bar{\lambda}-8\bar{\nu}-23}}}{2R_0}$$

$$k_{\mathrm{III},1} = k_{\mathrm{IV},1} = \frac{\sqrt{1-2\bar{\lambda}-4\bar{\nu}+\sqrt{4(\bar{\lambda}^2+4\bar{\nu}^2)+16\bar{\lambda}\bar{\nu}+12\bar{\lambda}-8\bar{\nu}-23}}}{2R_0}$$

$$k_{\mathrm{III},2} = \frac{\sqrt{1-2\bar{\lambda}-4\bar{\nu}-\sqrt{4(\bar{\lambda}^2+4\bar{\nu}^2)+16\bar{\lambda}\bar{\nu}+12\bar{\lambda}-8\bar{\nu}-23}}}{2R_0}$$

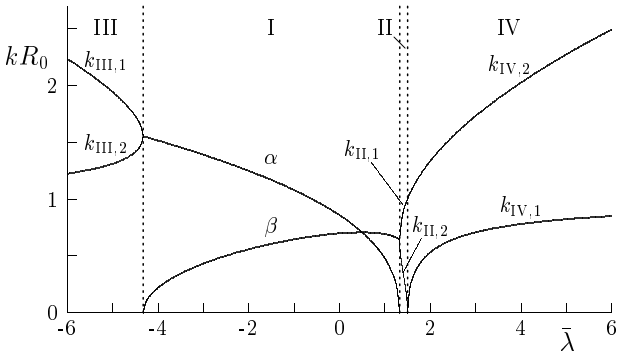

Fig. 4. The dependence of the product of the wave numbers (or their real and imaginary components for domain I) and the radius of the cylinder on the dimensionless lateral tension ($\bar{\lambda} = \lambda R_0^2/k_c + C_0^2 R_0^2/2$) for $\bar{\nu} = 0$. Curves $k_{\mathrm{III},1}$ and $k_{\mathrm{III},2}$ show the absolute values of the wave numbers if the parameter $\bar{\lambda}$ is smaller than $-\sqrt{8}-1.5$ (domain III). Curves α and β show the absolute values of the real and of the imaginary component of the product kR_0 if the parameter $\bar{\lambda}$ ranges between $-\sqrt{8}-1.5$ and $\sqrt{8}-1.5$ (domain I). Curves $k_{\mathrm{II},1}$ and $k_{\mathrm{II},2}$ show the absolute values of the wave numbers in the range of the parameter $\bar{\lambda}$ between $\sqrt{8}-1.5$ and 1.5 (domain II). Curves $k_{\mathrm{IV},2}$ and $k_{\mathrm{IV},1}$ show the absolute values of the wave numbers if the parameter $\bar{\lambda}$ is above 1.5 (domain IV). The dotted lines indicate different domain boundaries.

in general described as a linear combination of two even and two odd basic functions. The phase diagram shows the type of these basic functions in dependence on the parameters $\bar{\lambda}$ and $\bar{\nu}$. The corresponding wave numbers and the components of the wave numbers are given in Table 1. In domain I the deviation of the membrane shape from the cylinder is a sinusoidal function with exponentially decreasing amplitude (damped undulation). In domain II the shape of the membrane is described by the sum of exponential functions involving two different characteristic lengths. In domain III the shape of the membrane is the sum of two sinusoidal functions. In domain IV the deviation is given by the sum of a sinusoidal function and an exponential function. The obtained types of basic functions indicate that the values of the parameters $\bar{\lambda}$ and $\bar{\nu}$ for long close to ideal tubelike shapes lie in domains I or II where deviations from the cylinder decrease exponentially.

In Figure 3 the region of positive pressure differences is divided from the region of negative pressure differences by the dashed curve C. Furthermore, after expressing equation (12) in terms of the dimensionless parameters ($\bar{\lambda}$ and $\bar{\nu}$), we can obtain an equation for the dependence of the axial force (f) on these dimensionless parameters. The obtained equation shows that negative axial forces are below the line for $f = 0$ (the dashed line D) in the phase diagram and that positive forces are above it.

In order to better conceive the predicted behavior of nearly cylindrical membrane sections, the wave numbers, or their real and imaginary components, are presented in Figure 4 as a function of $\bar{\lambda}$ for a constant value of $\bar{\nu}$ ($\bar{\nu} = 0$). It can be seen that the transitions between different shape domains exhibit a variable behavior with respect to merging, branching, vanishing or arising of the real and imaginary components of the wave numbers. The nearly cylindrical shapes belonging to domains I and II are realized at values of $\bar{\lambda}$ around zero. At larger dimensionless lateral tensions, where the difference between the inside and the outside pressure is positive, there is a tendency in the system for the increase of the volume per length of the cylindrical section. At pressure differences larger than k_c/R_0^3 (within domain IV) this tendency causes a sinusoidal deformation of the cylindrical section because more volume can be accommodated under a given membrane area in the case of sinusoidal deformation. This effect is analogous to the Rayleigh instability [27] in the sense that a large positive pressure difference can be reduced by the sinusoidal deformation. At sufficiently negative dimensionless lateral tensions the axial force is negative and there is a tendency for shortening the vesicle section due to the action of the compressing axial force. Within domain III, *i.e.*, at axial forces smaller than $-\sqrt{8}\pi k_c/R_0$ for $\bar{\nu} = 0$, thus, the tendency in the system for shortening the vesicle section also causes the cylindrical section to deform sinusoidally.

The dependence of shapes of the nearly cylindrical sections on the difference between the lateral tensions of the membrane monolayers ($\bar{\nu}$) can be interpreted in a similar manner. The sinusoidal deformation mainly occurs at negative values of $\bar{\nu}$ (domain III in Fig. 3). Because in most parts of domain III the force is negative, the reason for this deformation can be the compressing axial force, as already discussed. However, at negative values of $\bar{\nu}$, the sinusoidal deformation may arise also due to the tendency of the system to increase the difference between the areas

of the outer and the inner monolayer (ΔA). Namely, the difference between the lateral tensions of the monolayers (ν) increases proportionally by increasing ΔA (Eq. (2)). Within domain III a large negative difference between the lateral tensions can be then reduced by the sinusoidal deformation of the cylindrical section because the area difference between the monolayers per length of the cylindrical section is larger for the waved tubular section than for the cylinder. This effect can be related to the already discussed occurrence of the sinusoidal deformation at large positive pressure differences. There the pressure difference is reduced whereas here the difference between the lateral tensions is reduced upon the deformation. The importance of the latter effect is clearly evidenced at the values of the parameters lying between curves A, B and D in Figure 3 where the negative difference between the lateral tensions can be reduced by the sinusoidal deformation even if the axial force is positive.

4 Conclusions and an application

In this work we studied first the dependence of the radius of the nearly cylindrical section on parameters defining the system's conditions (μ, λ and ν). The radius of these sections depends only on the pressure difference (μ) and the lateral tension (λ) (Eq. (9)) because the area difference, which is a conjugated parameter to the difference between lateral tensions (ν), does not depend on the radius of the cylinder. However, the radius of the reference cylinder can be also expressed by the equation that relates all three system parameters with the axial force (f) (Eq. (10)). From the demonstrated interdependence between the pressure difference and the lateral tension at given ν and f in Figure 1 we can infer what are the separate relations between μ, λ, ν and f. At fixed pressure difference and lateral tension the relation between ν and f is simple in that the difference between the lateral tensions and the axial force are related linearly.

We also determined the limitations for possible values of the parameters. For the positive pressure difference between the inner and the outer medium the nearly cylindrical sections exist only at sufficiently large values of the lateral tension (expression (11)). At positive pressure differences and sufficiently large lateral tensions there are two possible radii for the cylindrical sections. The analysis presented does not give any formal limitations for the value of the difference between the lateral tensions of the membrane monolayers (ν). However, if ν is too large, the membrane certainly disintegrates. Otherwise, we can estimate the typical value of ν in the tether pulling experiments by using equation (2). From given values for the nonlocal bending modulus, the area of the vesicle membrane and the distance between the neutral surfaces of the monolayers ($k_{\mathrm{r}} = 4.1 \times 10^{-19}$ J, $A = 10^3$ μm^2 and $h = 2.8$ nm [13]), the estimated value of ν, for the tether length of 100 μm, is in the order of 10^{-4} N/m. This value of ν is of the same order of magnitude as a change in the lateral tension (λ) in these experiments [13].

Then we determined the basic functions for the shapes of nearly cylindrical axisymmetric sections of vesicles for a complete variety of possible system's conditions defining the behavior of the system (μ, λ and ν). The different types of shape deviations depend on all three parameters but the values for the wave numbers can be expressed by only two independent parameters (cf. Eq. (13)). A possible convenient way to describe the different types of deviations is to express the dimensionless product of complex wave numbers and cylinder radius (kR_0) in terms of the parameters $\bar{\lambda}$ and $\bar{\nu}$ that define a combination of the system's conditions (Tab. 1). The shape equation (Eq. (3)) that determines the basic functions describes the possible stationary axisymmetric configurations of membranes. Thus, at given values of the parameters the described shapes do not necessarily correspond to stable configurations.

The analysis presented provides the analytical description of nearly cylindrical, axisymmetric shapes for an arbitrary length of the cylindrical vesicle section. This analytical description can also be discussed in relation to the stability analysis of long cylinders [17]. For long cylindrical vesicle sections, the deviation from the cylinder within domains I and II (Fig. 3), where the deviation of the membrane shape from a cylinder is described by a sinusoidal function with exponentially decreasing amplitude and by the sum of exponential functions involving two different characteristic lengths, respectively, is negligibly small throughout most of the length of the cylindrical section. This result is in accord with the result of stability analysis since the range of parameters for domains I and II, where long cylindrical sections are expected, coincides with the range of parameters, where the long cylinders are stable with respect to axisymmetric deformations [17]. Our analysis confirms the existence of long cylinders in domains I and II, and additionally shows that the cylinders adjust to the rest of the vesicle by exponential (domain II) or damped undulatory (domain I) deviations.

We also predicted the shapes of nearly cylindrical vesicle section within domains (domains III and IV in Fig. 3) where the long cylinders were shown to be unstable towards axisymmetric deformations [17]. In domain IV the shape deformation of the central part of a long tubular section can be described by a sinusoidal function with a single wavelength, whereas in domain III the shape deformation consists of two sinusoidal functions with two different wavelengths. At the ends of the tubular section, in domain IV the ajustment of the shape deformation to the rest of the vesicle is described by exponential function.

Because we limit ourselves only to the study of axisymmetric shapes, the analytical description for nearly cylindrical shapes may not be generally applicable. It was shown that at certain values of parameters long cylinders are unstable towards nonaxisymmetric deformations [17, 18]. In our phase diagram (Fig. 3) the regions of this kind of instabilities for long cylinders are below the zero force line (the dashed line D) and for $\bar{\lambda} < -2.5$. Hence, a long tubular section described by a sum of two sinusoidal functions exists only in a small region between curves A, B and

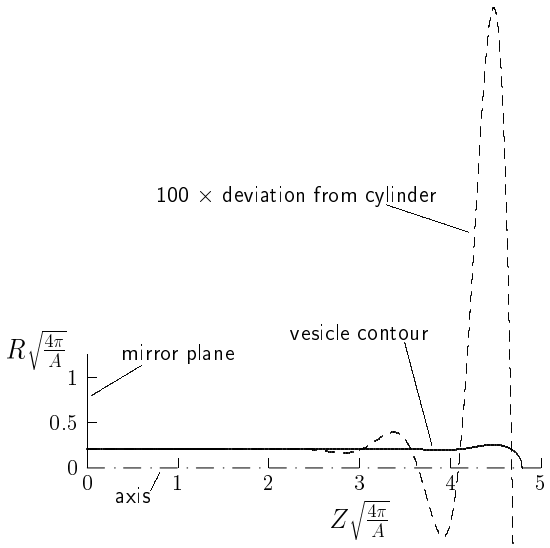

Fig. 5. The shape of a vesicle with the relative volume (vesicle volume divided by the volume of a sphere enclosed by the membrane of the same area A) 0.306. The vesicle axial cross-section (full line) is represented by the upper part of the contour for one half of the vesicle exhibiting equatorial mirror symmetry. The dashed curve represents enlarged deviation of the contour from the reference cylinder $(100 \times (R(Z) - R_0) + R_0)\sqrt{4\pi/A}$, where $R_0 = 0.2042\sqrt{A/(4\pi)}$. The contour of the vesicle was obtained by numerically solving [1] equation (3) for $\nu = 0$ and $C_0 = 0$.

D in Figure 3, and a long tubular section described by a single sinusoidal function exists in domain IV only above curve D.

The phenomena of the sinusoidal deformations of tubelike membrane sections are analogous to the Rayleigh instability. In the case of tubelike membrane sections, the elastic energy of the membrane is also an important factor. Our analysis points to a new possible cause for the occurrence of the instability. Namely, the tubelike membrane sections can be deformed sinusoidally also due to the altered difference between the lateral tensions of the membrane monolayers when the inner monolayer is more stretched than the outer one.

As already noted, the occurrence of a cylindrical section is a characteristic for vesicles with small relative volumes. Observed [11] as well as numerically obtained (Fig. 5) shapes of such vesicles have at both vesicle ends slightly wider rounded parts, and a nearly cylindrical middle part which at a closer look shows an undulatory behavior with a strongly decaying amplitude. The latter vesicle section can be described by the present analytical solutions. An advantage of the analytical description over the numerical one is in providing a quantitative insight into the vesicle shape behavior, which we shall briefly demonstrate.

The vesicle in Figure 5 was chosen to have zero difference between the lateral tensions and zero spontaneous curvature, *i.e.* $\nu = 0$ and $C_0 = 0$. Also, there are no forces applied and therefore $f = 0$. Then, by using equations (9) and (10), the value of the dimensionless lateral tension can be obtained, $\bar{\lambda} = -1.5$. The position of the obtained point ($\bar{\lambda} = -1.5$, $\bar{\nu} = 0$) within domain I (Fig. 3) explains the damped undulatory behavior obtained numerically. By having the value of $\bar{\lambda}$ for the treated vesicle, it is also possible to obtain the values of the products αR_0 and βR_0. By using the expressions presented in Table 1, we get $\alpha R_0 = 1.169$ and $\beta R_0 = 0.605$. We can compare the value of the product αR_0 with the approximate value obtained from the numerically calculated vesicle shape (Fig. 5). With the estimated values of the wavelength and the reference radius in the units $\sqrt{A/(4\pi)}$ (1.098 and 0.2042, respectively), we obtain that the approximate value of the product αR_0 is also 1.169. Furthermore, for $\bar{\lambda} = -1.5$, the predicted ratio between two consecutive amplitudes is $\exp(-2\pi\beta/\alpha) = 0.0387$, which is again in agreement with the shape presented in Figure 5. On the other hand, the present analysis does not include the determination of the amplitudes of the undulatory behavior. It has to be realized that these amplitudes depend on the characteristics of the noncylindrical parts of the vesicle.

The agreement between the analytical and the numerical description suggests that it is possible to obtain the contour of the tubular vesicle with small relative volume by having the numerical solution for the nearly cylindrical middle part replaced by the analytical solution. In this case, only rounded parts at the vesicle ends are to be solved numerically. In general, the usual numerical metods for solving the differential equation for the whole tubular vesicles become at larger lengths of their middle part extremely sensitive to the initial guesses of adjustable parameters. By the prescribed numerical and analytical approach it is possible to obtain the shapes of tubular vesicles for arbitrary small relative volumes, and thus to extend the shape analysis to include regions of the phase diagram where numerical methods have failed.

Other cases where the present analysis of nearly cylindrical sections may provide additional insights include different processes in which cylindrical membrane shapes transform into noncylindrical ones, as it occurs when pulling on a tubular vesicle [28] or when asymmetrically varying the areas of bilayer monolayers [29]. In the detailed analysis of such processes the specific external conditions have to be taken into consideration, however, this is outside the scope of this work.

References

1. S. Svetina, B. Žekš, in *Handbook of Nonmedical Applications of Liposomes 1995*, edited by D.D. Lasic, Y. Barenholz, Vol. **I** (CRC, Boca Raton, FL, 1996) p. 13.
2. U. Seifert, Adv. Phys. **46**, 13 (1997).
3. H.J. Deuling, W. Helfrich, J. Phys. (Paris) **37**, 1335 (1976).
4. S. Svetina, B. Žekš, Eur. Biophys. J. **17**, 101 (1989).
5. U. Seifert, K. Berndl, R. Lipowsky, Phys. Rev. A **44**, 1182 (1991).
6. F. Jülicher, U. Seifert, Phys. Rev. E **49**, 4728 (1994).

7. W. Helfrich, Z. Naturforsch. C **29**, 510 (1974).
8. E.A. Evans, Biophys. J. **14**, 923 (1974).
9. M. Kraus, U. Seifert, R. Lipowsky, Europhys. Lett. **32**, 431 (1995).
10. B. Božič, S. Svetina, B. Žekš, Phys. Rev. E **55**, 5834 (1997).
11. E. Farge, P.F. Devaux, Biophys. J. **61**, 347 (1992).
12. R.M. Hochmuth, H.C. Wiles, E.A. Evans, J.M. McCown, Biophys. J. **39**, 83 (1982).
13. R.E. Waugh, J. Song, S. Svetina, B. Žekš, Biophys. J. **61**, 974 (1992).
14. N. Benlimame, D. Simard, I.R. Nabi, J. Cell Biol. **129**, 459 (1995).
15. J.W. Dai, M.P. Sheetz, Biophys. J. **68**, 988 (1995).
16. Ou-Yang Zhong-can, W. Helfrich, Phys. Rev. A **39**, 5280 (1989).
17. D.J. Bukman, Jian Hua Yao, M. Wortis, Phys. Rev. E **54**, 5463 (1996).
18. Zhang Shao-guang, J. Phys. Soc. Jpn. **68**, 3603 (1999).
19. Ou-Yang Zhong-can, W. Helfrich, Phys. Rev. Lett. **59**, 2486 (1987).
20. S. Svetina, M. Brumen, B. Žekš, Stud. Biophys. **110**, 177 (1985).
21. S. Svetina, B. Žekš, Eur. Biophys. J. **21**, 251 (1992).
22. L. Miao, U. Seifert, M. Wortis, H.-G. Döbereiner, Phys. Rev. E **49**, 5389 (1994).
23. Hu Jian-Guo, Ou-Yang Zhong-can, Phys. Rev. E **47**, 461 (1993).
24. R. Podgornik, S. Svetina, B. Žekš, Phys. Rev. E **51**, 544 (1995).
25. V. Heinrich, B. Božič, S. Svetina, B. Žekš, Biophys. J. **76**, 2056 (1999).
26. Wei-Mou Zheng, Jixing Liu, Phys. Rev. E **48**, 2856 (1993).
27. Lord Rayleigh, Philos. Mag. **34**, 145 (1892).
28. R. Bar-Ziv, E. Moses, P. Nelson, Biophys. J. **75**, 294 (1998).
29. D.L. Tanelian, V.S. Markin, Biophys. J. **72**, 1092 (1997).